Experimental measurement and numerical simulation of the thermal performance of a double glazing system with an interstitial Venetian blind

Yanyi Sun, Yupeng Wu Robin Wilson and Sixu Lu*

Architecture and Built Environment, Faculty of Engineering, The University of Nottingham, University Park Nottingham, NG7 2RD, UK

**Corresponding author: Tel: +44 (0) 115 74 84011; emails: Yupeng.Wu@nottingham.ac.uk, Jackwuyp@googlemail.com*

Abstract

Venetian blinds, which were originally designed to provide sun shading and privacy, also have the potential to reduce heat transfer caused by internal and external temperature difference when integrated within the cavity between the two panes of a double glazing unit. In this paper, the thermal performance of a glazing system with and without a Venetian blind with various slat orientation angles under different temperature conditions are investigated by both experimental measurement (undertaken in a large climate chamber) and numerical simulation (obtained via Computational Fluid Dynamic modelling). The thermal resistance of Venetian blind glazing system varies with the change of slat inclination angle, and it also highly depends on the mean temperature of the glazing and the temperature difference between the indoor and outdoor environment. Inclusion of a Venetian blind modifies both the absolute and relative strengths of convection and radiation. Vertically oriented slats showed the most significant contribution to increasing radiative thermal resistance, which led to the best overall thermal performance. The system achieved up to a maximum of 28% improvement of U-value when compared with that of a glazing unit with the absence of a Venetian blind. Empirical correlations generated based on simulations could be used for future building energy simulation.

Key words: Venetian blind; Climatic Chamber; Computational Fluid Dynamics; Thermal Performance; Convection; Radiation.

Nomenclature

Symbols

A	aspect ratio $A = L/s$	-
$a - e$	coefficients for polynomial regression	-
c_p	specific heat capacity	J/kg·K
$Const.$	constant	-
d	thickness of glass pane	m
g	Gravitational acceleration	m/s^2
h	-heat transfer coefficient	$W/m^2 \cdot K$
	-also thermal conductance	$W/m^2 \cdot K$
L	length of the window air gap	m
n	number	-
q	Heat flux	W/m^2
R	Thermal resistance	m·K/W
s	width of the air gap	M
T	temperature	℃
U	thermal transmittance	$W/ m^2 \cdot K$
ΔT	temperature difference	℃
β	thermal expansion coefficient	1/K
ε	emissivity	-
λ	thermal conductivity	W/m·K
μ	dynamic viscosity of air	kg/m·s
ρ	density of air	kg/m^3
σ	Stefan-Boltzmann constant	$W/m^2 \cdot K^4$
$\emptyset$	slat orientation angle	°

Dimensionless Numbers

Gr	Grashof number
Nu	Nusselt number
Pr	Prandtl number
Ra	Rayleigh number

Subscripts

a	air
b	blind
c	control
e	external
g	glass
i	Internal
j	enumerate of individual measurement
m	mean
r	radiation
s	surface
t	total
w	wall

1. Introduction

Venetian blinds were originally designed to provide adjustable control of incoming solar radiation [1], and meanwhile allowing ventilation with window open. For this reason, the application of Venetian blind adjacent to windows shows an extensive popularity in regions with sufficient solar radiation in cooling-dominated climates [2]. More recently, Venetian blinds appears in the air cavity, between the two glazing panes of double glazed window units [3], and this kind of commercial fenestration product also spread in mild climate, such as United Kingdom. This development is driven not only by aesthetics and ease of maintenance, but also by the benefit that these interstitial Venetian blinds improves the thermal resistance of a window unit [4]. This is because when the slats of Venetian blind are in a horizontal position (as shown in Fig.4(b)), the interstitial walls of the cells provide additional viscous resistance to the onset of free convection and interfere with the thermal radiation transferred from one pane of the double glazed unit to the other. If the slats are in a vertical position, the cavity is divided longitudinally into two spaces by a septum as shown in Fig.4(d)). This has the potential to dramatically reduce the long-wave radiation heat transfer between the two glass panes.

For the purpose of improving the performance of glazing systems and hence improving indoor comfort and achieving building energy conservation, a considerable volume of research reported in the literature focused on the application of advanced fenestrae systems or shading devices [5-9] in buildings, while other studies pay attention to the fundamental investigation of the optical and thermal characteristics of these fenestration systems [2, 4, 10-17]. Gomes et al [2] used net radiation method to determine the transmitted, reflected and absorbed solar and visible radiation of glazing with venetian blinds at different inclined angles. Asdrubali et al. [18] and Chen et al. [10] used a hot box method to investigate thermal transmittance of different complex fenestration systems. Laser interferometry has been used to obtain temperature field visualization and hence to analyse the convection in complicated glazing units with different internal blinds [11-

13]. These experimental techniques have been accompanied by numerical studies that have proved indispensable in exploring the complicated building elements. Computational Fluid Dynamics (CFD) tools have been used by researchers to solve the heat transfer problem and explore the air flow pattern in the vertical air cavity of conventional double-glazing unit [19-23]. Zhao et al.[19] Wright et al. [21] and Ganguli et al. [22, 23] used finite volume method to study the natural convection in the cavity of double-glazing units. They concluded that with the increase of temperature difference, multi-cellular flow developed, which tends to increase the convective heat transfer coefficient. There has been some work undertaken to investigate the possibility of reducing free convection by integrated shading devices, such as windows with horizontal Venetian blind, pleated blind and different configurations of fins [3, 14-17] into the cavity. However, in most of these studies, long-wave radiation heat transfer, which accounts for two thirds of the total heat transfer through the air cavity [20], is neglected in the numerical modelling. Although improved simulation methods have been implemented by Avedissian and Naylor [15], who used a surface-to-surface model to include radiation, they only used the model to calculate the U-value of the whole system instead of evaluating the effects of the internal structure on long-radiative heat transfer. Although, the thermal resistance of the glazing system varies with the change of the system mean temperature of the glazing and the temperature difference between the two glazing panes, detailed investigations of the interstitial Venetian blinds on the reduction of heat transfer in terms of both convection which is driven predominately by temperature difference across the two glass panes, and radiation which is driven predominately by glazing system mean temperature under different environmental conditions that commonly encountered in buildings are less conducted. Consequently, the design limitation and specific requirements for the building application of interstitial Venetian blinds are not drawn clearly.

This study aims to explore the thermal characteristics of a double glazing unit with and without a Venetian blind installed in the air cavity between two glazing panes. The experimental results were used to validate the numerical model and the validated numerical model was then used to investigate the thermal performance of the glazing system with different slat orientation angles under different temperature conditions and incident solar radiations. Instead of studying the U value of glazing systems under a standard condition, simulation were undertaken over a range of different mean temperatures of two glazing panes and a range of temperature differences between the surfaces to allow a comprehensive picture of convective and radiative heat transfer to be established, and their effects on window thermal resistance/ U value. The results of these studies were used to generate empirical correlations for the thermal resistance of double glazing with Venetian blind between glazing panes.

2. Experimental investigation

Experimental studies of the selected glazing systems were carried out at the Laboratory at the Energy Technology Building, University of Nottingham. Double glazing units with and without a Venetian blind were completed under a series of controlled temperature conditions. The experimental apparatus, the glazing units and the measurement procedure are described in this section.

2.1 The climatic chamber

The thermal performance of the glazing units was measured in a TAS series 2 LTCL600 climatic chamber as shown in Fig.1. The Climate Chamber comprises two insulated walk-in rooms (both are 4m×3.5m×2.6m) providing a steady and cyclic simulation of climatic environment. Each enclosure can be individually controlled and thus it is possible to simulate external climate conditions in one, whilst the other mimics internal conditions. One of the rooms is physically fixed while the other maybe wheeled to one side to allow the construction of a 'Test Wall'. Once constructed, the two rooms were brought together to sandwich the 'Test Wall'. During the test, integral air conditioning units can be used to control the temperature of the two rooms within the range from -25℃ to +60℃ and the relative humidity between 10% to 95%. Various parameters, such as surface temperature, air temperature and heat flux of the ‘Test Wall’, can be obtained during operation.

Fig.1. (a) External view of the climatic chamber (b) Internal view of the chamber and air conditioning unit

2.2 Test samples

Two glazing units of size 1200mm× 1200mm×28mm were tested. One was a normal double glazing unit composed of two 4mm-thick low iron panes and a 20mm-wide cavity filled with air (labbelled as ‘DG’ in preceding discussions). The other was a double glazing unit with a Venetian blind installed in the air cavity between the two glazing panes (shown in Fig.2(a)). The slats were made of aluminium with a thickness of 0.25mm and width of 11mm. During the tests, two configurations were tested: one with the slats horizontal (tilt angle of 0° to the horizontal, labelled as ‘V0’ in preceding discussions) and the other with the slats vertical (tilt angle of 90° to the horizontal, labelled as ‘V90’).

2.3 The apparatus setup

The measurement method followed International Standard ISO 9869-1:2014 for In-situ thermal resistance measurements by using heat flow meters [24]. The apparatus setup was informed by International Standard ISO 12567-1:2012 for the determination of window and door thermal transmittance using the hot-box method [25]. Fig.2(b) shows a schematic cross-section of the test apparatus. A 300mm-thick insulated wall (with a measured U-value less than 0.3 W/m^{2}K) was sandwiched between the two rooms to form the initial 'Test wall'. The glazing units were then mounted in an aperture cut in the centre of the wall and at least 860mm away from the inside ceiling, floor or walls of the two rooms. The internal surface of the glazing unit was mounted flush with the surface of insulated wall according to ISO 12567-1:2012 [25]. Silicone sealant covered with tape was used around the joints between the window and the insulated wall in order to seal all gaps and hold the window firmly in position. In order to diminish the effect of convection caused by the fans on the air conditioning units, two baffles made from plywood were set in both the interior and exterior chambers, respectively. The distance between the baffles and surfaces of the insulated wall, in which the testing glazing units were installed, was 500mm.

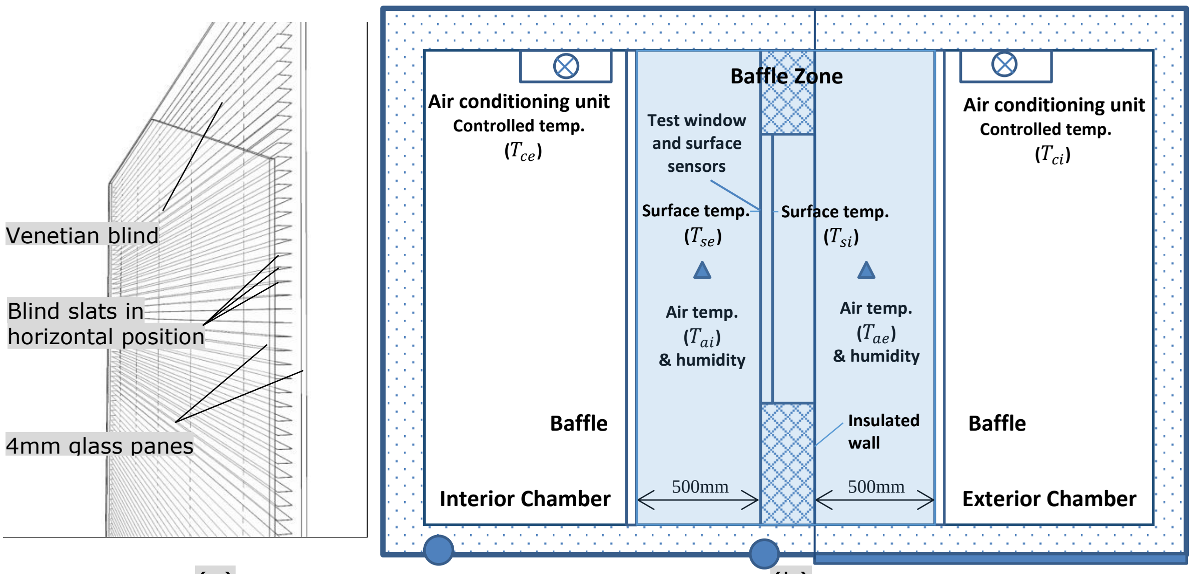

(a) (b)

Fig.2. (a) Schematic of the double glazing unit with Venetian Blind, the slats are horizontally placed (V0) (b) View of the system, the test specimen and sensors

Eighteen T type thermocouples (Fig.3) with detector diameter less than 0.3mm were attached on each side of the window unit [25] to measure external and internal surface temperature (labelled as T_{se} and T_{si} shown in Fig.2(b), respectively). Heat flux meters (Hukesflux Type HFP01, with thermal resistance <6.25 × 10^{-3} m^{-2}K/W, measurement accuracy +/-5%) were affixed to the glass by a thin layer of thermal contact paste (Servisol, with thermal conductivity 0.77 W/mK) [24] for heat flux (q) measurement. The thermal resistance of the heat flux meters is low enough for the effects of perturbation of the surface heat flow by positioning the heat flux meter to be assumed negligible. Two temperature and humidity probes CS215 (accuracy +/-0.4℃ for temperature and +/-2% for humidity) were used to measure the air temperature (labelled as T_{ae} and T_{ai} shown in Fig.2 (b)) and humidity in the two baffles spaces beside the window. Two hot wire air velocity sensors (testo 425, with measurement accuracy +/- 0.03m/s) were used to monitor the air velocities within the baffle zone. The thermocouples, heat flux meters and temperature and humidity probes are connected to a 24-channel data logger DT85 which logged data at 1 minute intervals.

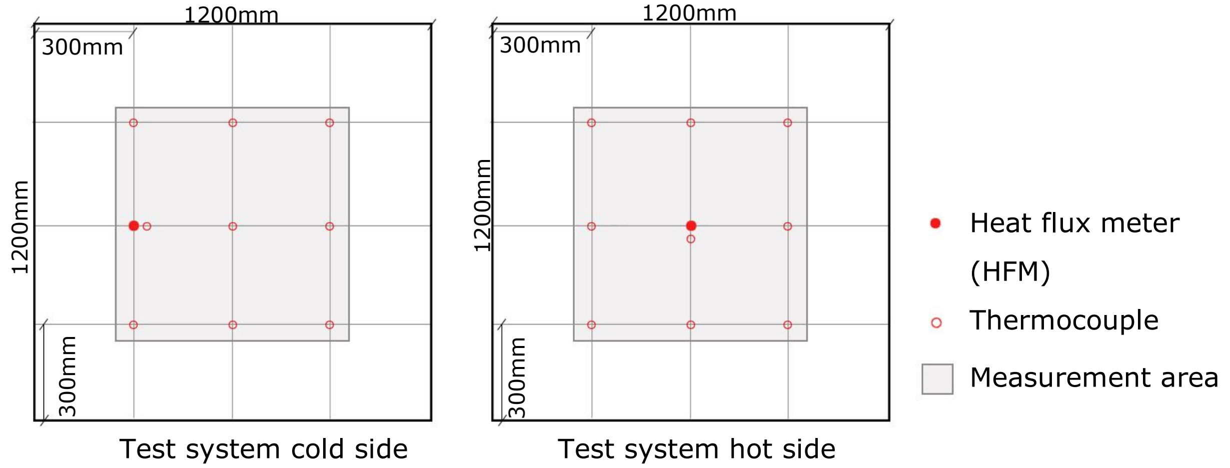

Fig.3. Detailed view illustrating the locations of the thermocouples and heat flux meters on the surfaces of the glazing unit

2.4 Measurement procedure and data acquisition

Before the test, the instrumentation (i.e. thermocouples) calibrations were conducted. At the beginning of the test, 6 heat flux meters and over 30 thermocouples were placed inside and around the measurement area (Fig.3) of the glazing surface to verify the uniformity of surface temperature and heat flux. The results showed uniform reading in the measurement area (see Fig.3) and the extra 4 heat flux meters and thermocouples are removed to reduce their perturbation.

As both the glazing unit mean temperature and the temperature difference between the panes of the unit affect heat transfer, when testing the window samples five pairs of controlled temperature settings (T_{ce} and T_{ci} for exterior and interior chamber, respectively) were set to the air conditioning units. The five scenarios aim to achieve an arrangement of designed surface temperatures

(T_{se} and T_{si}) of the two glazing panes, as shown in Table 1. Scenarios 1-3 aimed to keep the mean temperature of the glazing unit to be constant at 10°C, but vary the surface temperature difference between the two glazing panes from 7°C to 15°C. Scenarios 4 and 5 sought to keep the surface temperature difference between the two glazing panes is the same as scenario 3 (15°C), and vary the mean temperature between 7°C and 14°C. However, the controlled temperatures (T_{ce} and T_{ci}) were only applied to the air conditioning units outside the baffle spaces (Fig.2(b)), continuously testing of the settings on the air conditioning units required until the surface temperatures (T_{si} and T_{se}) on the glass reach the desired value as shown in Table 1. To avoid condensation, the relative humidity in the interior room was set at 30%. The measured wind speed is less than 0.3m/s to represent natural convection prevails [25].

Table 1: Arrangement of mean temperature and surface temperature difference of 5 scenarios for glazing systems

Scenario No.	1	2	3	4	5
Mean temperature of glazing unit (T_m) (°C)	10	10	10	7	14
Surface temperature difference between two glazing panes ($T_{si} - T_{se}$) (°C)	7	11	15	15	15

Generally, tests were run for a sufficient duration (over 72 hours) to allow the environmental conditions in the test rooms and the heat flow through the window to stabilise for each scenario, and then the measured data over a further period of 48 hours were used for analysis.

2.5 Analysis of the data

The glazing surface temperature (T_{se} and T_{si}) and heat flux (q) were measured during the experimental test and average method was used to analyse the data [24] and obtain the thermal resistance of the glazing system by using Equation (1):

$$R_T = \frac{\sum_{j=1}^{n}(T_{sij} - T_{sej})}{\sum_{j=1}^{n} q_j} \quad (1)$$

where the index *j* enumerates the individual measurement.

The heat transmittance, *U*, can be obtained from Equation (2):

$$U = \frac{\sum_{j=1}^{n} q_j}{\sum_{j=1}^{n}(T_{aij} - T_{aej})} \quad (2)$$

The thermal resistance of the normal double glazing unit obtained through experiment was compared with the calculated values determined according to EN673 [26], as well as simulation results using CFD. The measurement results of the glazing unit with Venetian blind were also compared with CFD simulation results. The standard calculation method and numerical simulation approach are detailed described in Section 3 and the measured and predicted results are compared in Section 5.2.

3. Theoretical investigation

3.1 Standard calculation

The recognised method for the calibration of experimental measurements on double or multiple glazing, is to compare the test result of a normal double glazing unit with results obtained using the standard calculation method EN673:2011[26]. The total thermal transmittance between two glazing panes consists of radiative heat transfer (h_r) and the heat transmittance through the air by convection and conduction (h_a). According to the empirical equation set out in EN673:2011[26], the radiation conductance h_r is given by:

$$h_r = 4\sigma(\frac{1}{\varepsilon_1} + \frac{1}{\varepsilon_2} - 1)^{-1}T_m^3 \tag{3}$$

where σ is the Stenfan-Boltzmann's constant, T_m is the mean absolute temperature of the gas space, ε_1 and ε_2 are the corrected emissivity of the surfaces bounding the enclosed space between the panes at the T_m.

And the heat transmittance of air cavity is given by:

$$h_a = Nu\frac{\lambda}{s} \tag{4}$$

where s is the width of the air space, λ is the thermal conductivity of the air space, and the Nusselt number Nu is given by:

$$Nu = Const.(Gr \cdot Pr)^n \tag{5}$$

where the value of $Const.$ and n for vertical glazing are 0.035 and 0.38 respectively. The Nusselt number, which represents the ratio between the pure conduction resistances to a convection resistance [27], is an important dimensionless coefficient that indicates the intensity of convection. It is affected by three dimensionless parameters. They are aspect ratio of the cavity, the Prandtl number and the Grashof number of the fluid. The aspect ratio ($A = \frac{L}{s}$) describes the geometry of the air cavity. The Prandtl number ($Pr = \frac{c_p \mu}{\lambda_a}$) describes the ratio of momentum diffusivity to thermal diffusivity. The Grashof number ($Gr = \frac{g \beta \Delta T s^3 \rho^2}{\mu^2}$) describes the relationship between buoyancy and viscosity within a fluid. The Rayleigh number (Ra), which is the product of Grashof number and Prandtl number, can be regarded as the ratio of buoyancy and viscosity forces multiplied by the ratio of momentum and thermal diffusivities.

3.2 Computation Fluid Dynamic simulation

This section presents the main features of the numerical model employed to reproduce the experimental test. Two-dimensional finite volume models were developed in the commercial CFD package FLUENT. The thermal performance of a double glazing unit with a Venetian blind at four different configurations (slats horizontally placed (V0), slats vertically placed (V90), slats at tilted angles of $\emptyset = 30°$ (V30), and $\emptyset = 60°$ (V60)) to the horizontal were investigated. The air cavity of the glazing system has a width of 20mm and length of 1200mm. The schematic diagrams of the normal double glazing system and glazing system with slats at various angles are illustrated in Fig.4.

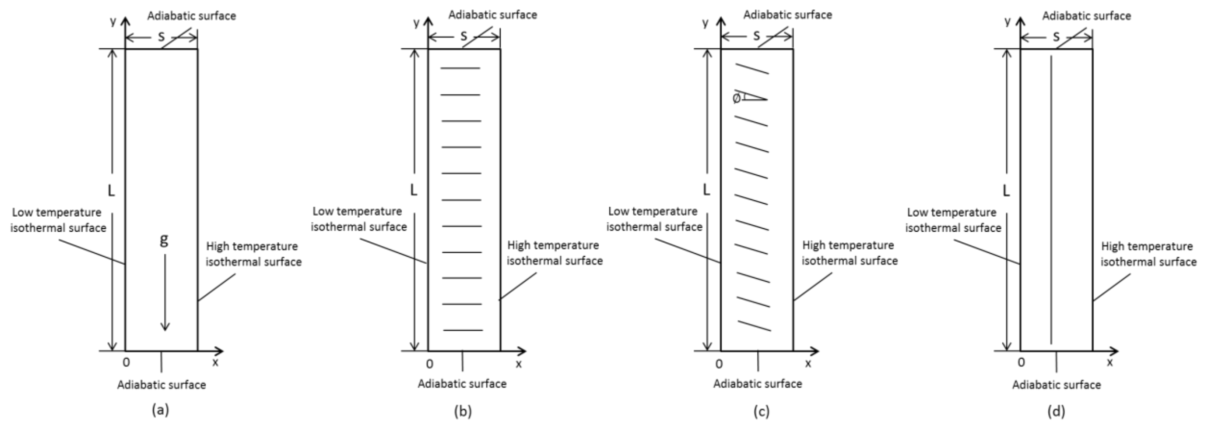

Fig.4: (a) 2D schematic diagram illustrating the geometry of the glazing system without blind (b) glazing system with horizontally placed slats (c) glazing system with the inclined slats (d) glazing system with vertically placed slats

To simplify the CFD simulation process, the following assumptions were made: 1) the internal surfaces of the left and right glass panels were set as two isothermal walls with different temperatures to represent the temperature difference between indoor and outdoor environments, while the top and bottom ends were assumed to be adiabatic; 2) the enclosure was filled with air with Pr = 0.71, all thermophysical properties (e.g. c_p, λ) of the fluid were assumed to be constant [14, 15, 17], except for the fluid density and viscosity, which vary with temperature. The flows in the vertical cavity or cells remain laminar, because the Grashof Numbers never reach the related critical value [3]. The Surface to Surface (S2S) radiation model was used to solve the radiative transfer equation. The boundary conditions of the two isothermal surfaces were set to match the mean temperature and surface temperature difference, used in the experimental study.

In order to account for the boundary layer effect, the mesh size was defined as smaller near the boundaries and the slats (0.025mm×0.025mm), and then gradually increased toward the centre of the air cavity. Extensive mesh independent studies were undertaken. Iterative convergence was achieved when the normalized residuals were less than 10^{-3} for the continuity, and 10^{-7} for the energy and momentum equations. The estimated result of local convective heat flux and combined convective and radiative heat flux were calculated from the converged temperature field.

It needs to be mentioned that, when considering the effect of solar radiation on the convection within the air cavity, the slats are assumed to have an absorptivity/emissivity equals to

0.1 which is a common value of a high reflective aluminium Venetian blind [28], and thus an average heat flux of 25 W/m^2, 50 W/m^2 and 75W/m^2 are applied on the slat to represent the low, medium and high horizontal irradiation, respectively.

The thermal conductance (R) of a double glazing unit with and without Venetian blind structures can be expressed in equation (6):

$$R = \frac{\Delta T}{(\frac{\partial T}{\partial x})_w \lambda_a} = \frac{\Delta T}{q} \quad (6)$$

where $(\frac{\partial T}{\partial x})_w$ is the air temperature gradient on the wall and q is the average heat flux of combined convective and radiative heat transfer across the two surfaces. ΔT(℃) is the temperature difference between the hot and cold surfaces of the glazing system.

The results of convective heat flux at the boundaries were used to express the local Nusselt number (*Nu*) as follows:

$$Nu = \frac{(\frac{\partial T}{\partial x})_w s}{\Delta T} = \frac{qs}{\lambda_a \Delta T} \quad (7)$$

4. Measurement results and validation

The results from the experimental tests are presented in this section along with an explanation of how they were used to validate the CFD model.

4.1 Experimental results

The measured data: air temperatures; surface temperatures; heat fluxes, and the calculated mean temperatures; temperature differences; Rayleigh number; surface to surface thermal resistances and U-values for 3 different configuration systems (DG, V0 and V90) under 5 scenarios which are described in table 1 are shown in Tables 2, 3 and 4.

Table 2: The thermal performance of the double glazed unit (DG)

No.	T_{ai} (°C)	T_{ae} (°C)	ΔT_a (°C)	T_{si} (°C)	T_{se} (°C)	$\overline{T_s}$ (°C)	ΔT_s (°C)	Ra	q (W/m^2)	R (m·K/W)	U (W/ m$^2 \cdot$ K)
DG-1	19.5	2.5	17.0	14.7	7.2	11.0	7.5	7393.7	39.3	0.191	2.312
DG-2	22.3	-3.1	25.4	15.4	4.3	9.9	11.1	10942.7	58.4	0.190	2.299
DG-3	23.9	-4.3	28.2	16.3	3.9	10.1	12.4	12224.3	65.4	0.189	2.319
DG-4	19.7	-4.8	24.5	13.7	1.7	7.7	12.0	12323.6	61.9	0.193	2.526

DG-5	25.7	-3.9	29.6	17.7	4.9	11.3	12.8	12365.4	68.7	0.186	2.321

Table 3: The thermal performance of the double glazing system with venetian blind, where the slats are horizontally placed (V0)

No.	T_{ai} (°C)	T_{ae} (°C)	ΔT_a (°C)	T_{si} (°C)	T_{se} (°C)	$\overline{T_s}$ (°C)	ΔT_s (°C)	Ra	q (W/m²)	R (m·K/W)	U (W/ m² · K)
V0-1	17.1	2.5	9.8	13.9	6.3	10.1	7.7	7590.9	32.4	0.237	2.219
V0-2	21.4	-1.4	10.0	16.5	4.6	10.6	11.9	11731.4	50.1	0.238	2.198
V0-3	24.9	-5.6	9.6	18.1	2.47	10.3	15.6	15379.0	65.6	0.238	2.150
V0-4	20.8	-6.4	7.2	14.2	0.4	7.4	13.8	14172.1	57.4	0.240	2.112
V0-5	29.1	-0.9	14.1	21.8	6.7	14.3	15.1	13735.2	65.8	0.229	2.193

Table 4: The thermal performance of the double glazing system with venetian blinds, where the slats are vertically placed (V90)

No.	T_{ai} (°C)	T_{ae} (°C)	ΔT_a (°C)	T_{si} (°C)	T_{se} (°C)	$\overline{T_s}$ (°C)	ΔT_s (°C)	Ra	q (W/m²)	R (m·K/W)	U (W/ m² · K)
V90-1	15.9	4.5	10.2	13.9	7.0	10.4	6.9	6802.2	20.5	0.336	1.797
V90-2	18.9	0.8	9.8	15.9	4.8	10.3	11.0	10844.2	32.3	0.340	1.784
V90-3	22.6	-3.6	9.5	17.8	2.5	10.1	15.3	15083.2	45.3	0.337	1.729
V90-4	19.2	-5.2	7.0	15.0	0.3	7.7	14.6	14993.7	42.0	0.347	1.72
V90-5	27.8	1.6	14.7	23.0	7.3	15.1	15.7	14281.0	47.6	0.329	1.820

In each test, the climate chamber worked constantly for a long period to keep the system in a steady state. Fig.5 shows the test data for the double glazing unit scenario 3 (DG-3) for the first 22 hours. It may be seen that the temperature and heat flux tend towards a constant value after approximately 7 hours of testing, indicating that steady state condition had been achieved. The fluctuation is less than 0.5 °C for the temperature and it is approximately +/-3 W/m² for the heat flux.

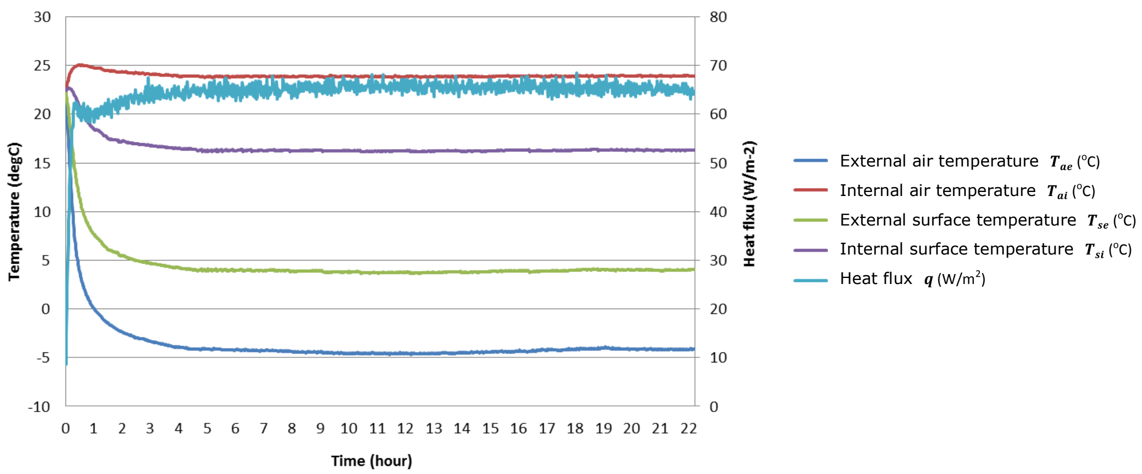

Fig.5: Example of climate chamber measurement (DG-3) of the first 22 hours.

4.2 Comparison between experimental test, standard calculation and CFD

For double glazing unit (DG), the results based on the calculation method set out in EN673 [26] were compared with measured results. In addition, the measured results of the glazing system with and without Venetian blinds were also compared with the results obtained by CFD simulation to validate the accuracy of CFD modelling. Fig.6 (a) shows the first 3 scenarios of each system, in which, the mean temperature of the tests are kept at 10°C and with an increase of temperature difference from 7°C to 15°C, the average heat flux of all these three structures increase. For example, the heat flux of DG increases from approximately 40 W/m^2 to 65 W/m^2. The average heat flux obtained from CFD simulation shows a difference of less than 1.2% for DG and less than 2.7% for V0 and V90 when compared with the experimental results. Similarly, Fig.6 (b) shows the relationship between average heat flux and mean temperature for a constant temperature difference of each system. Increasing mean temperature results in an increase of the heat flux (e.g. from approximately 43 W/m^2 to 48 W/m^2 for V90). Both the CFD simulation and the calculated results match well with the experimental results, the differences are less than 1% for the double glazing unit and less than 4% for the glazing unit with blinds (V0 and V90).

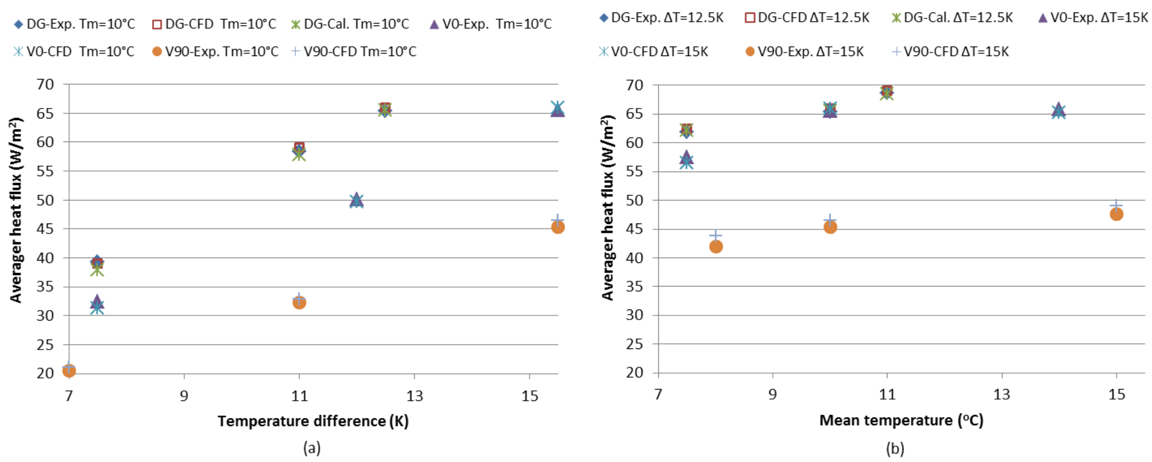

Fig.6: Measured, calculated and simulated heat flux through glazing system (a) Scenarios 1, 2 and 3 in DG V0 and V90; (b) Scenarios 3, 4 and 5 in DG V0 and V90

The comparison between these three methods provides a degree of confidence in the CFD modelling, which means further model developed using this method may be used to extend the thermal analysis of the glazing system with Venetian blinds.

5. CFD simulation results and discussion

Further analysis of the performance of the glazing unit with Venetian blinds was undertaken using the validated numerical model. During the simulation, the slats were arranged at four different configurations: horizontally placed (V0), vertically placed (V90), titled at 30° (V30) and 60° (V60) to the horizontal. Firstly, the variations of convection within the region between two glazing panes with different configurations are investigated under temperature only and combination of temperature and incident solar radiation conditions, respectively. Then, the thermal resistance of these systems under various temperature conditions are undertaken. Empirical correlations for the thermal resistance are also generated.

5.1 Convection within the region between two glazing panes

Fig.7 shows the stream function contours and partial enlarged drawings of the velocity vector for different configurations at the mean temperature of 10°C with a temperature difference of 15°C. The effect of incident solar radiation has not been considered over here and the convection is only driven by the temperature difference between the two glazing panes.

In the double glazing unit (DG, Fig 7 (a)), the fluid travels upwards near hot side surface, and downwards adjacent to the cold side surface, where it is being cooled. As the Rayleigh Number is larger than the critical value, secondary cells start to present [29]. Vertically placed slats (V90, Fig 7 (d)) stop the presence of secondary cells by forming two cavities with higher aspect ratio, and induce the air to flow in a large single circle. The horizontally placed slats (V0, Fig 7 (b), on the other hand, induce the air to recirculate within the cells between two slats. Due to the increased viscous resistance caused by the slats, the intensity of convection dramatically reduced. The inclined slats (V30 and V60) have the combined effects of the vertical and horizontal configurations. In which, the air mainly flows in large circle but there still is very weak recirculation in the cells. V60 have the most stagnant fluid because part of the air flow is blocked between slats. The effects of these different configurations on the overall convective performance are shown in Fig.8.

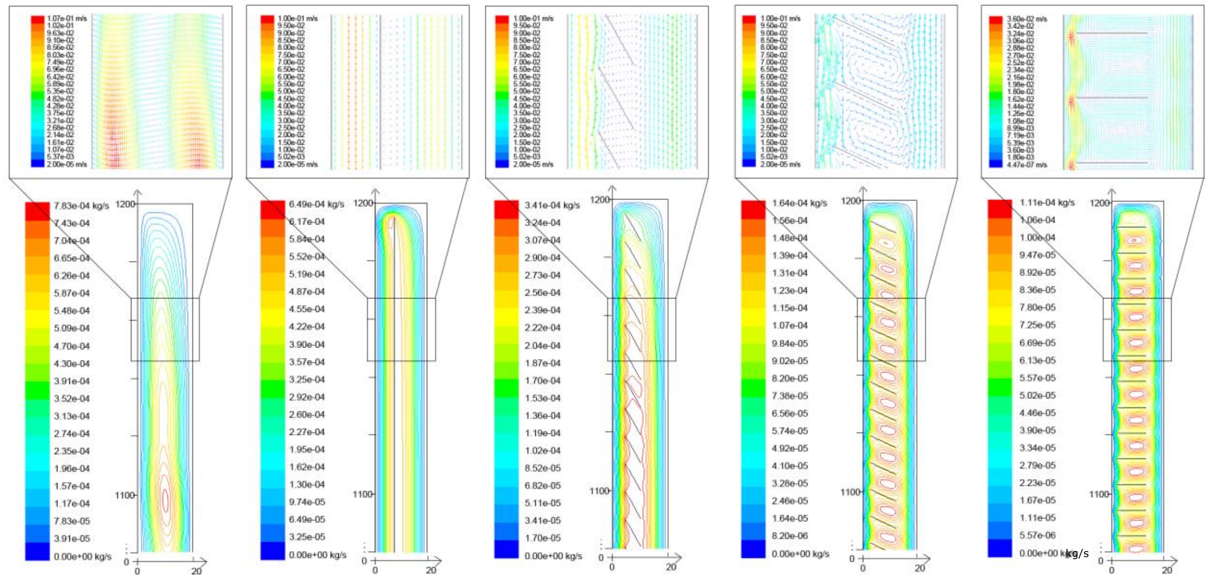

(a) DG (b) V90 (c) V60 (d) V30 (e) V0

Fig.7: Stream function and velocity vector at $\overline{T_s} = 10$°C, $\Delta T_s = 15$°C for different configurations, Ra=14736.2

The Nusselt number is an important dimensionless coefficient that indicates the intensity of convection, which changes from 1.1 to 1.8 across these five configurations over the full range of the Rayleigh numbers studied. When the Rayleigh number is less than 10^4 , the Nusselt number in all configurations is less than 1.2, which indicates that the convective heat transfer is not significant [30]. When the Rayleigh number increases above 10^4, convection has a more significant effect in the double glazing unit (DG) than that in the horizontal (V0), vertical (V90) and 30^o titled slats (V30). The unit with the slats at an inclination angle of 60^o (V60), having the smallest Nusselt number, provides the best effect of convection reduction caused by an increase of combined viscous resistance for the large circle and recirculation within cells.

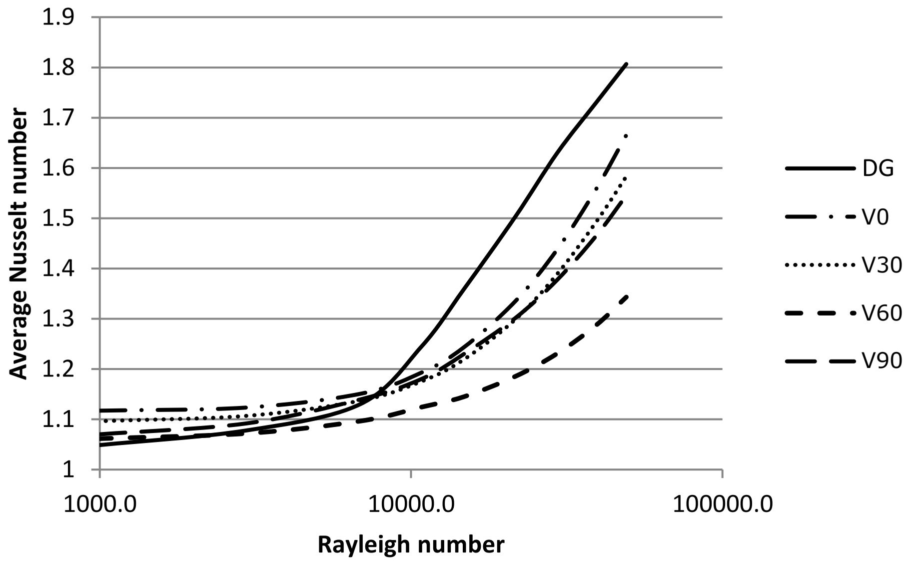

Fig.8: Effect of blind configurations on the average Nusselt number at different Rayleigh number

When the effect of incident solar radiation absorbed by the slats is taken into consideration, the convection within the region between two glazing panes is determined by the combination effect of solar radiation and glazing temperature. Figs.9 and 10 show the combination effect of absorbed solar radiation and temperature difference between the two glazing panes on the convection with Venetian blind at 30° titled (V30). When there is no incident solar radiation (Figs.9 (a) and (i)), the buoyance-driven natural convection is purely caused by the temperature difference between the two glazing panes, and the slats capture the air flow and forced air recirculate in the cells. On the other hand, when there is no temperature difference between the two glazing panes as shown in Figs.9 (e) and (v), the slats that are heated by absorbed solar radiation have the highest temperature in the region. Temperature difference between the slats and the two glazing panes causes a bidirectional flow pattern, but the convection intensity is weak. The conduction becomes the dominate heat transfer mechanism and thermal bridging effect between the slat tips and the glazing panes results in a peak values of the local heat flux (120 W/m^2) as shown in Fig.10. Because the distance between the slats and the left glazing pane is much shorter than that at the right hand side, therefore, heat transfer rate through left glazing pane and its fluctuation are much greater than that of the right glazing pane. When both the temperature difference and the absorbed solar radiation exist, the flow pattern is mainly depended on the intensity of absorbed solar radiation. For the case illustrated in Fig.9, when absorbed solar radiation is 25 W/m^2, the slats reach a temperature similar to the hot glazing pane, and hence there is no obvious heat transfer on the hot side, the heat flux is only 3 W/m^2. But on the cold side, as the temperature difference between the slats and the cold glazing pane increases significantly when compared with the case of no radiation, the local convective heat transfer rate also enlarges to an average value of 51.2 W/m^2. When increasing the absorbed solar radiation from 25 W/m^2 to 75 W/m^2, the convection continually increases and the bidirectional flow pattern becomes more obvious. From Fig.10, it also can be found that with increase of the convection, the thermal bridging effect is reduced, and thus the fluctuation of local convective heat flux becomes more flat.

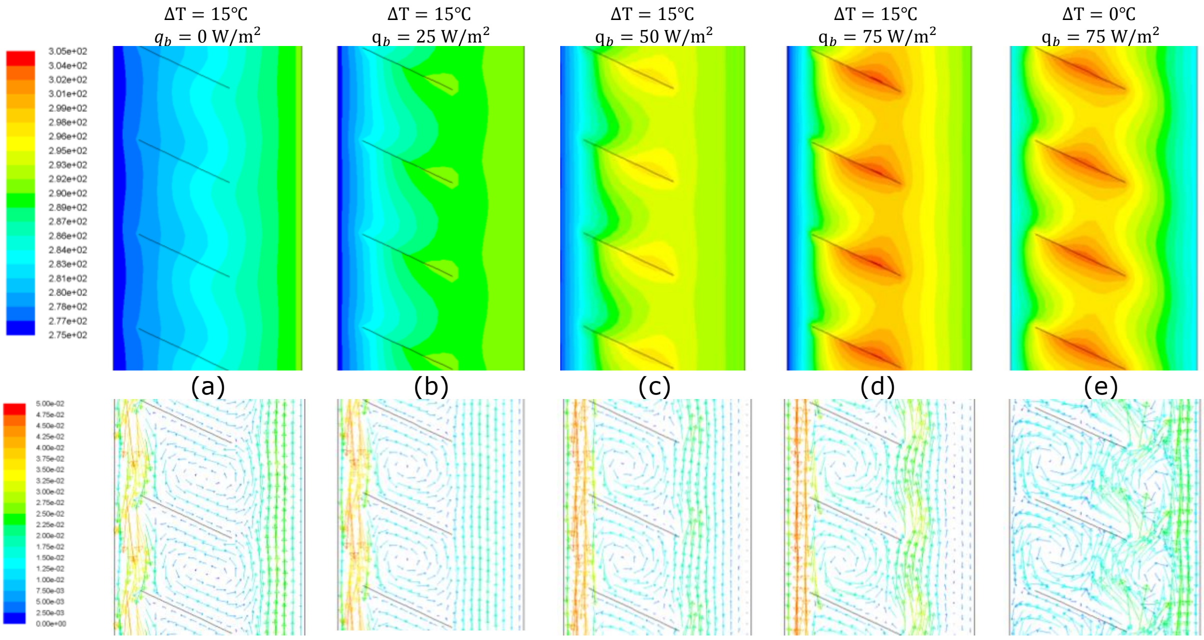

Fig.9: Temperature contours (a)-(e) and velocity vectors (i)-(v) of V30: (a) and (i) $\Delta T = 15℃, q_b = 0W/m^2$; (b) and (ii) $\Delta T = 15℃, q_b = 25W/m^2$; (c) and (iii) $\Delta T = 15℃, q_b = 50W/m^2$; (d) and (iv) $\Delta T = 15℃, q_b = 75W/m^2$; (e) and (v) $\Delta T = 0℃, q_b = 75W/m^2$

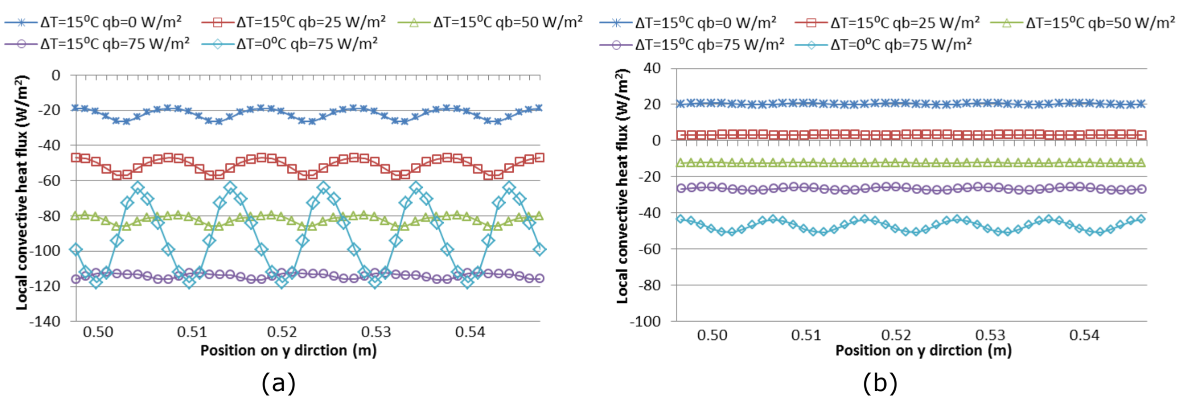

Fig.10: Local convective heat flux on (a) left glazing pane, cold side (b) right glazing pane, hot side

The average local heat flux on glazing panes under various glazing temperatures and incident solar radiations is shown in Table 5. When taking the solar radiation effect into consideration, the distance between the slat tips and the glazing panes becomes an important factor that influence the heat flux on the glazing surfaces. Moreover, the change of titled angle (e.g. from 30° to 60° when q_b=75 W/m^2) might result in an obvious change of flow pattern and hence result in the convective heat transfer increase on one side and decrease on the other side. The heat flow direction depends on the interrelationship between the slat absorbed solar radiation and glazing surface temperature.

Table 5: Average local heat flux (W/m^2) at left and right glazing panes of V0, V30 and V60 under different temperature and solar radiation conditions.

	$q_b = 0$ W/m^2		$q_b = 25$ W/m^2		$q_b = 75$ W/m^2				$q_b = 75$ W/m^2	
	left $T_s = 2.5$°C	right $T_s = 17.5$°C	left $T_s = 2.5$°C	right $T_s = 17.5$°C	left $T_s = 2.5$°C	right $T_s = 17.5$°C	left $T_s = 17.5$°C	right $T_s = 2.5$°C	left $T_s = 10$°C	right $T_s = 10$°C
V0	-22.9	21.1	-55.5	5.0	-121.5	-26.2	-62.5	-81.0	-93.0	-52.1
V30	-22.2	20.4	-51.3	3.1	-114.0	-26.5	-62.4	-75.3	-91.8	-47.2
v60	-20.6	18.7	-42.4	15.2	-97.7	-40.8	-66.7	-70.3	-88.0	-51.3

5.2 Radiative and convective thermal resistance analysis

In order to evaluate the thermal resistance of the glazing system, only variation of temperature conditions are considered in this section. The simulated thermal resistance of double glazing unit with and without Venetian blinds at various surface temperature differences and different mean temperature are shown in Fig.11. For the double glazing unit with a constant mean temperature, when the surface temperature difference increases from 0°C to 30°C, the thermal resistance reduces by 13.5%. Meanwhile, for a same temperature difference, with the increase of mean temperature from 0°C to 20°C, the thermal resistance reduces by approximately 14%. The remaining configurations show a similar trend which is most significant for the vertically oriented slats (V90) as the mean temperature and temperature difference can vary the thermal resistance by 27%.

As both the mean temperature of the glazing units and the temperature difference across the glazing panes have effects on the thermal resistance of the glazing systems, and the trend of each configuration is similar, a polynomial regression, Equation (8), was used to correlate the data. The regression coefficients for the fit are given in Table 5:

$$R = a - bT_m - c\Delta T + dT_m\Delta T + e\Delta T^2 \quad (8)$$

where T_m is the mean temperature of the two glass panes (°C) and ΔT is the temperature difference between two glass panes (°C).

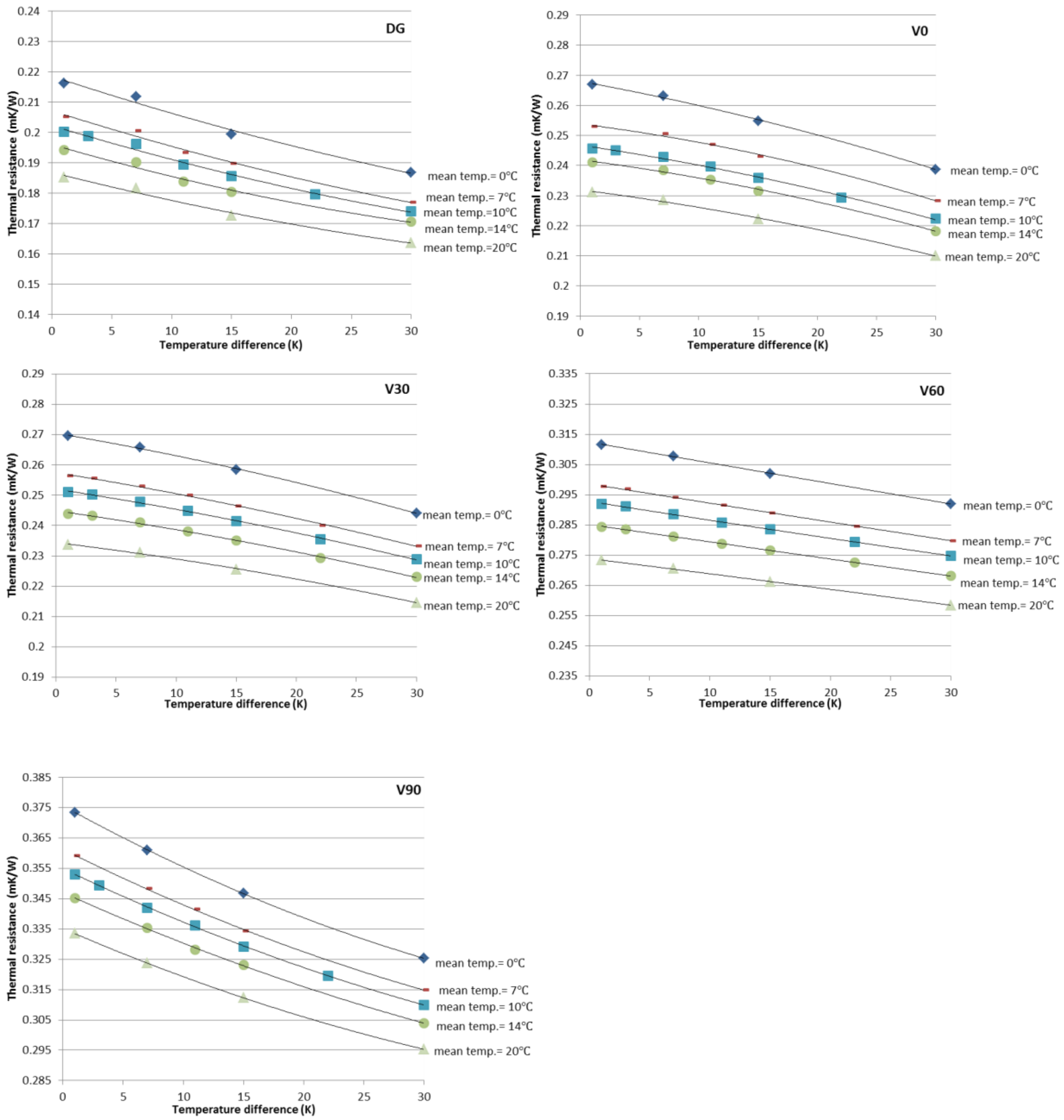

Fig.11: Comparison between CFD simulation and equation calculation at same mean temperature and various temperature differences

Table 6: Coefficients for the polynomial regression predicting thermal resistance of different configurations (Eq. 12)

	a	b	c	d	e
DG	0.2183	0.0016	0.00133	10^{-5}	10^{-5}
V0	0.2668	0.0017	0.00068	10^{-5}	-10^{-5}
V30	0.2703	0.0018	0.0007	10^{-5}	-6×10^{-6}
V60	0.3122	0.0019	0.0007	10^{-5}	10^{-6}
V90	0.3754	0.002	0.0022	2.6×10^{-5}	10^{-5}

The temperature difference has less of an influence on the thermal resistance of the configuration of horizontal and tilted slats (V0, V30 and V60) than that of the other two configurations (DG and V90), as the slopes of the trend lines for V0, V30 and V60 (which is **c** shown in Table 6) are smaller than that of DG and V90. This indicates that convection in V0, V30 and V60 driven by the temperature difference between the two glass panes reduces more effectively than that in cavities without blind or with a vertically placed blind. This is because the slats in V0, V30 and V60 configurations capture fluid mass to keep it recirculating within the cells reducing the fluid carrying heat and reducing the convection heat transfer and increase resistance.

To explore the effects of the mean temperature and the temperature difference on the total thermal resistance of glazing units, heat transfer caused by the radiation and convection have been decoupled from the overall heat flux. As shown in Fig.12, the radiative heat transfer is the dominant heat transfer mechanism, accounting for 50%-72% of the total in all the structures. Thus, a significant reduction of radiative heat transfer due to the presence of the Venetian blind results in a significant reduction in the total thermal conductance. The vertically placed blind (V90), which reduces the radiative heat transfer by over 72% as compared with that of the DG configuration, shows the best reduction in radiative heat transfer. Although, the V60 configuration has the best convection reduction, which is 1.43 W/m^{2}K, however, radiative heat transfer represents a significant heat transfer path, which makes the total thermal conductance of V60 higher than that of V90.

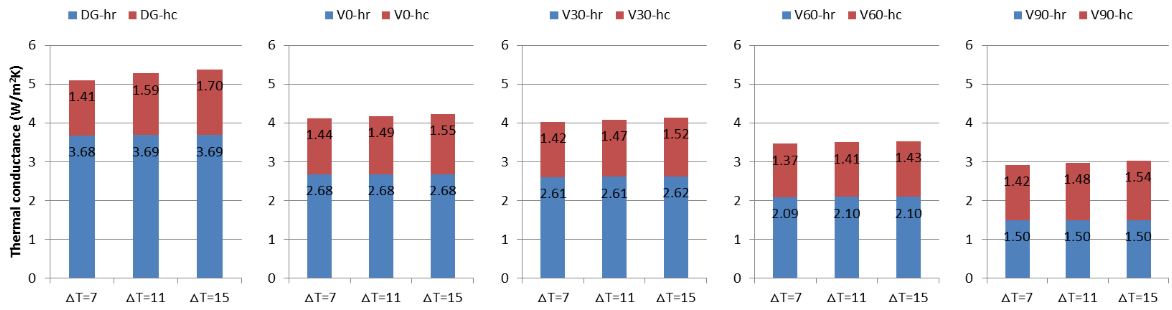

(a) $T_m = 10°C$, $\Delta T = 7°C, 11°C \;\&15°C$

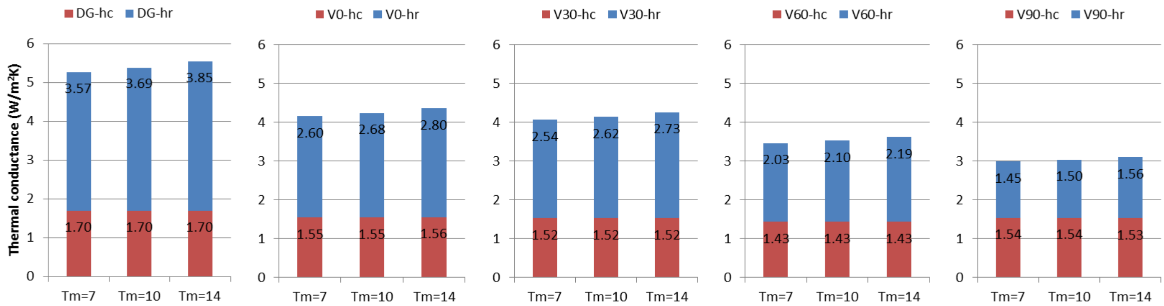

(b) $\Delta T = 15°C$, $T_m = 7°C, 10°C \;\&14°C$

Fig.12: Thermal conductance caused by radiation (hr) and convection (hc) for different configurations at (a) a constant mean temperature 10℃ (b) a fixed temperature difference of 15℃

5.3 Total thermal resistance and U-value

The overall heat transfer of the glazing system under standard boundary conditions EN 673 [26] (temperature difference of 15℃ between two glazing panes, average glazing panes temperature of 10°C) was simulated and discussed in this section. Fig.14 illustrates the total thermal resistance ($R_t = \frac{1}{U}$), which is the sum of the thermal resistance between two glass panes ($\frac{1}{h}$), the glass panes thermal resistance ($\frac{2d}{\lambda_g}$) and the external and internal surfaces thermal resistance ($\frac{1}{h_e}$ and $\frac{1}{h_i}$). The U-values of double glazing with and without Venetian blind configurations are shown in Table 6.

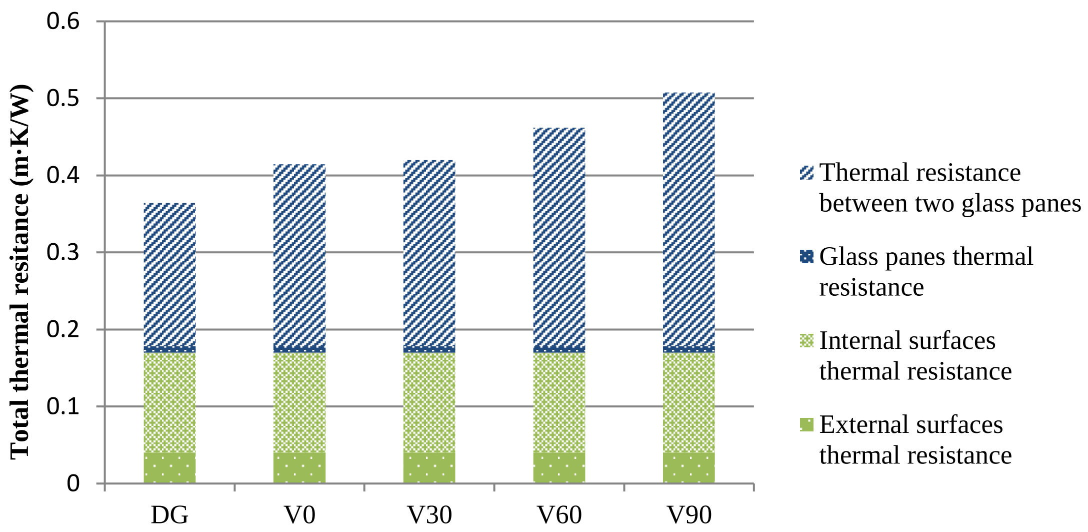

Fig.13. Total thermal resistance (R_t) of different configurations of window unit with Venetian blinds with individual resistance contributions

Table 7 U-values of different configurations of window unit with Venetian blind configurations

	DG	V0	V30	V60	V90
U-value (W/m^{2}K)	2.747	2.413	2.382	2.165	1.970

From Fig.13 and Table 7, it can be seen that, as the surface thermal resistances and glass panes thermal resistance are assumed constant in all these structures, adding a Venetian blind leads to an increase of thermal resistance between the two glazing panes and hence a reduction of the U-value. The thermal resistance between two glazing panes only contributes to approximately 50% of the total thermal resistance in the normal double glazing unit (DG). When the slats are in their vertical position (V90), the thermal resistance is significantly increased. This yields a 28% reduction of the U-value. Meanwhile, horizontally placed (V0), 30^o titled (V30) and 60^o titled (V60) slats can yield a 12%, 13% and 22% improvement in U-value, respectively.

6. Conclusion

A comprehensive investigation of the thermal performance of the glazing system with a Venetian blind was conducted using experiment and CFD simulation. Experimental results, simulation results and calculation results agree well with each other, and this provides a degree of confidence over further use of the numerical model to explore the thermal characteristics of interstitial Venetian blind at various slats inclination angles under different conditions. The following conclusions can be drawn: 1) interstitial Venetian blind can effectively reduce the convective heat transfer in the air gap of a double glazing unit; 2) for glazing system with interstitial blind, convection is also affected by the solar radiation that absorbed by slats; 3) the convective thermal resistance, which is driven by temperature difference between two glazing panes, can affect the overall thermal resistance by 13.3-14% in common climatic conditions ($1℃ \leq \Delta T \leq 30℃$); 4) the radiative thermal resistance, which is driven predominately by mean temperature of the panes, has a significant effect on the overall thermal conductance and it can affect the thermal resistance by 10.6-13.5% in the temperature range commonly encountered in buildings ($0℃ \leq \bar{T} \leq 20℃$); 5) in general, the presence of interstitial Venetian blind at different slat titled angle can achieve 12% to 28% improvements in U-value when compared with that of a normal double glazing unit.

Acknowledgements

This work was supported by the Faculty of Engineering, University of Nottingham and the China Scholarship Council through a joint PhD studentship to Yanyi Sun.

Reference

[1] Tian C, Chen T, Chung T-m. Experimental and simulating examination of computer tools, Radlink and DOE2, for daylighting and energy simulation with venetian blinds. Applied Energy. 2014;124:130-9.
[2] Gomes MG, Santos AJ, Rodrigues AM. Solar and visible optical properties of glazing systems with venetian blinds: Numerical, experimental and blind control study. Building and Environment. 2014;71:47-59.
[3] Dalal R, D. Naylor, Roeleveld D. A CFD study of convection in a double glazed window with an enclosed pleated blind. Energy and Buildings. 2009;41:1256-62.
[4] Shahid H, Naylor D. Energy performance assessment of a window with a horizontal Venetian blind. Energy and Buildings. 2005;37:836-43.
[5] Huang Y, Niu J-l, Chung T-m. Comprehensive analysis on thermal and daylighting performance of glazing and shading designs on office building envelope in cooling-dominant climates. Applied Energy. 2014;134:215-28.
[6] Ihara T, Gustavsen A, Jelle BP. Effect of facade components on energy efficiency in office buildings. Applied Energy. 2015;158:422-32.
[7] Singh R, Lazarus IJ, Kishore VVN. Effect of internal woven roller shade and glazing on the energy and daylighting performances of an office building in the cold climate of Shillong. Applied Energy. 2015;159:317-33.

[8] Roetzel A, Tsangrassoulis A, Dietrich U. Impact of building design and occupancy on office comfort and energy performance in different climates. Building and Environment. 2014;71:165-75.
[9] Blanco JM, Arriaga P, Rojí E, Cuadrado J. Investigating the thermal behavior of double-skin perforated sheet façades: Part A: Model characterization and validation procedure. Building and Environment. 2014;82:50-62.
[10] Chen F, Wittkopf SK. Summer condition thermal transmittance measurement of fenestration systems using calorimetric hot box. Energy and Buildings. 2012;53:47-56.
[11] Almeida F, Naylor D. Experimental study of free convection in a window with a heated between-panes blind. Energy and Buildings. 2011;43:2647-55.
[12] Naylor D, Lai BY. Experimental Study of Natural Convection in a Window with a Between-Panes Venetian Blind. Experimental Heat Transfer. 2007;20:1-17.
[13] Wright JL, Jin H, Hollands KGT, Naylor D. Flow visualization of natural convection in a tall, air-filled vertical cavity. International Journal of Heat and Mass Transfer. 2006;49:889-904.
[14] Giorgi LD, Bertola V, Cafaro E. Thermal convection in double glazed windows with structured gap. Energy and Buildings. 2011;43:2034-8.
[15] Avedissian T, Naylor D. Free convective heat transfer in an enclosure with an internal louvered blind International Journal of Heat and Mass Transfer. 2008;51:283-93.
[16] Naylor D, Collins M. Evaluation of an Approximate Method for Predicting Theuvalue of a Window with a between-Panes Blind. Numerical Heat Transfer, Part A: Applications. 2005;47:233-50.
[17] Collins M, Tasnim S, Wright J. Numerical analysis of convective heat transfer in fenestration with between-the-glass louvered shades. Building and Environment. 2009; 44:2185-92.
[18] Asdrubali F, Baldinelli G. Thermal transmittance measurements with the hot box method: Calibration, experimental procedures, and uncertainty analyses of three different approaches. Energy and Buildings. 2011;43:1618-26.
[19] Zhao Y, Curcija D, Gross WP. Prediction of multicellular flow regime of natural convection in fenestration glazing cavities. ASHRAE Transactions. 1997;103:1-12.
[20] Gan G. Thermal transmittance of multiple glazing: computational fluid dynamics prediction. Applied Thermal Engineering. 2001;21:1583-92.
[21] Wright JL, Sullivan FF. A two-dimensional numerical model for natural convection in a vertical rectangular window cavity. ASHRAE Transactions. 1993;99:1193-206.
[22] Ganguli AA, Pandit AB, Joshi JB. CFD simulation of heat transfer in a two-dimensional vertical enclosure. Chemical Engineering Research and Design. 2009;87:711-27.
[23] Ganguli AA, Pandit AB, Joshi JB. Numerical predictions of flow patterns due to natural convection in a vertical slot. Chemical Engineering Science. 2007;62:4479-95.
[24] Standardization IOf. ISO 9869-1: 2014 Thermal insulation -- Building elements -- In-situ measurement of thermal resistance and thermal transmittance Part 1: Heat flow meter method. 2014.
[25] Standardization IOf. ISO 12567-1:2012 Thermal performance of windows and doors -- Determination of thermal transmittance by the hot-box method -- Part 1: Complete windows and doors. 2012.
[26] EN 673 Glass in building-- Determination of thermal transmittance (U value) – Calculation method. European standard2011
[27] Duffie JA, Beckman WA. Solar engineering of thermal processes. 3rd ed. Hoboken, N.J. : Wiley; 2006.
[28] Andersen M, Rubin M, Powles R, Scartezzini JL. Bi-directional transmission properties of Venetian blinds: experimental assessment compared to ray-tracing calculations. Solar Energy. 2005;78:187-98.
[29] Korpela SA, Lee Y, Drummond JE. Heat transfer through a double pane window. ASME Journal of Heat Transfer. 1982;104:539-44.
[30] Lee Y, Korpela SA. Multicellular natural convection in a vertical slot. J Fluid mech. 1983;126 91-121.